Available online at www.sciencedirect.com
SCIENCE DIRECT
Polymer 46 (2005) 3927–3935
polymer
www.elsevier.com/locate/polymer

Transient uniaxial orientation of flexible polymer chains in a wide range of elongation rates

Andreas Schoene[a,*], Andrzej Ziabicki[b], Leszek Jarecki[b]

[a]Mechanics and Fibre Formation, Leibniz Institute of Polymer Research Dresden, Hohe Strasse 6, 01069 Dresden, Germany
[b]Institute of Fundamental Technological Research, Polish Academy of Sciences, Swietokrzyska 21, 00-049 Warsaw, Poland

Received 25 November 2004; received in revised form 23 February 2005; accepted 24 February 2005
Available online 7 April 2005

Abstract

Affine evolution of chain end-to-end vectors distribution function is derived analytically for non-linear polymer liquids subjected to uniaxial elongational flow, controlled by time-evolution of chain deformation coefficients. Peterlin approximation for non-Gaussian chain elasticity is applied, with Padè approximation for the inverse Langevin function. The approach enables calculations of transient molecular deformation coefficients in entire range of elongation rates and times.

Equations controlling time evolution of the molecular deformation coefficients in elongational flow are solved analytically with an assumption of dominating elongational component. The approach allows to decouple evolution equations and obtain an approximate closed form analytical formula describing time evolution of the molecular deformation with high accuracy, in particular at higher elongation rates, above the Gaussian limit.

Predictions of the analytical formula are compared with numerical computations to evaluate the approximation and ranges of its validity.

The analytical formula enables predicting evolution of average functions in non-linear systems, such as free energy, tensile stress, molecular orientation, etc. The formula is used to discuss molecular vs. macroscopic deformation in wide range of elongation rates and times, as well as evolution of stress, axial orientation factor, apparent elongational viscosity.

Keywords: Transient molecular deformation; Uniaxial elongational flow; Non-linear stress-orientation behaviour

1. Introduction

Chain deformation and segmental orientation produced during polymer processing determine ultimate physical and mechanical properties of polymeric solids. Time evolution of molecular deformation and orientation during processing affects kinetics of structure development (oriented crystallization, crystal orientation, etc.) and final properties of the products.

Strong chain extension and orientation produced at fast uniaxial flow deformations in fiber melt spinning or in solid state drawing result in high enhancement of mechanical properties. Model analysis of time evolution of molecular deformation and orientation in such systems should consider non-Gaussian chain statistics and finite chain extensibility.

Time evolution of the distribution $W(\mathbf{h},t)$ of chain end-to-end vectors in non-Gaussian systems has been considered in our earlier paper [1] in a wide range of deformation rates using the following continuity equation

$$\frac{\partial W}{\partial (Dt)} - \mathrm{div}\left\{ \nabla W + W\left[\frac{\nabla F_{\mathrm{el}}(h)}{kT} - \frac{\mathbf{Q}h}{D}\right]\right\} = 0 \tag{1}$$

The system is represented by non-Gaussian elastic Brownian dumbbels embedded in a viscous continuum and subjected to steady flow deformation characterised by a uniform and constant velocity gradient tensor, $\mathbf{Q}$. D is diffusion coefficient of the chain ends. The evolution equation accounts for flow convection, Brownian motion of the chain ends, and the non-linear inverse Langevin elastic force between the chain ends

$$\nabla F_{\mathrm{el}} = \frac{kT}{ah}\mathcal{L}^{*}\left(\frac{h}{Na}\right)\mathbf{h} \tag{2}$$

* Corresponding author. Tel.: +49 351 4658 336; fax: +49 351 4658 284.
E-mail addresses: aschoene@ipfdd.de (A. Schoene), aziab@ippt.gov.pl (A. Ziabicki), ljarecki@ippt.gov.pl (L. Jarecki).

0032-3861/$ - see front matter © 2005 Elsevier Ltd. All rights reserved.
doi:10.1016/j.polymer.2005.02.109

$\mathcal{L}^*$-inverse Langevin function, h/Na characterises chain extension, and N is number of Kuhn segments of length a in the chain.

Two asymptotic solutions of Eq. (1) have been discussed in papers [2,3]. For low chain mobility, the convection term $\mathbf{Q}/D$ dominates the elastic and Brownian forces, and the chain distribution follows exactly the macroscopic deformation of the viscous matrix with the instantaneous deformation gradient tensor $\exp[\mathbf{Q}t]$ up to full chain extension. The other asymptote has been obtained at large molecular mobility and/or long deformation times when steady-state distribution is approached. For flow deformations characterised by a symmetric tensor $\mathbf{Q}$, an asymptotic steady-state Boltzmann distribution has been obtained. Such an equilibrium distribution is controlled by the non-Gaussian elastic potential and a flow potential resulting from frictional interactions between the chains and the flowing medium.

Example solutions of Eq. (1) illustrating time evolution of the distribution $W(\mathbf{h},t)$ between the asymptotic distributions have been discussed in paper [1] for biaxial and uniaxial flow deformations. Peterlin approximation [4] has been used to represent the non-Gaussian elastic force between chain ends.

2. Chain distribution evolution in a uniaxial elongational flow

In Peterlin approximation the elastic force, Eq. (2), is expressed by a product of a linear Gaussian term and a coefficient $\bar{E}$ which represents non-linear elasticity of a chain with an average square end-to-end distance

$$\nabla F_{\mathrm{el}} \cong \frac{3kT}{Na^2}\bar{E}(\langle h^2\rangle)\mathbf{h} \tag{3}$$

where

$$\bar{E}(\langle h^2\rangle) = \frac{\mathcal{L}^*(\langle h^2\rangle^{1/2}/Na)}{3(\langle h^2\rangle^{1/2}/Na)} \tag{4}$$

For Gaussian chains we have $\bar{E}=1$.

With the Peterlin approximation, the evolution equation reduces to a form typical for Gaussian systems, but with the elastic force modified by the parameter $\bar{E}$

$$\frac{\partial W}{\partial(Dt)} - \mathrm{div}\left[\nabla W + W\left(\frac{3\bar{E}\mathbf{h}}{Na^2} - \frac{\mathbf{Q}h}{D}\right)\right] = 0 \tag{5}$$

where $\bar{E}$ which deviates from unity the more, the higher is deformation of chains in the system.

An analytical self-consistent solution of Eq. (5) was proposed for the transient distribution in paper [1] for biaxial and uniaxial flows, but it was deviating considerably from a more exact numerical one in a wide range of deformation rates and processing times. In the present paper we propose a new analytical solution for transient distribution function and time-dependent chain deformations produced in uniaxial elongational flow which fits the numerical solution nearly perfectly, in particular in the range of intermediate and high strain rates.

We discuss transient chain distribution and molecular deformation in a non-linear system subjected to steady uniaxial elongational flow. Uniform velocity gradient tensor and an incompressible viscous medium are assumed, with the stretching direction along the $i=3$ axis

$$\mathbf{Q} = q_3\begin{bmatrix} -1/2 & 0 & 0 \\ 0 & -1/2 & 0 \\ 0 & 0 & 1 \end{bmatrix} \tag{6}$$

For the uniaxial flow deformation, evolution Eq. (5) with the Peterlin approximation reduces to the following form in the explicit components x_i of the end-to-end vector, $\mathbf{h}$

$$\frac{\partial W}{\partial(Dt)} - \nabla^2 W - \left(\frac{\partial W}{\partial x_1}x_1 + \frac{\partial W}{\partial x_2}x_2\right)\left(\frac{3\bar{E}}{Na^2} + \frac{q_3}{2D}\right) - \frac{\partial W}{\partial x_3}x_3\left(\frac{3\bar{E}}{Na^2} - \frac{q_3}{D}\right) - \frac{9\bar{E}}{Na^2}W = 0 \tag{7}$$

where $\bar{E}$ represents the modulus of elasticity, in $3kT/Na^2$ units, of a chain with an average square end-to-end distance at the instance of time, $\langle h^2(t)\rangle$. The approximation introduces formal linearity of the elastic potential in non-linear systems, physically sensible in the entire range of chain extensions. In consequence, it is easy to check that the above evolution equation is satisfied by a peudo-affine distribution function at any instant of time

$$W(\mathbf{h},t) = \frac{\mathrm{const}}{\tilde{\lambda}_1^2(t)\tilde{\lambda}_3(t)}\exp\left[-\frac{3}{2Na^2}\left(\frac{x_1^2+x_2^2}{\tilde{\lambda}_1^2(t)} + \frac{x_3^2}{\tilde{\lambda}_3^2(t)}\right)\right] \tag{8}$$

where the time-dependent molecular elongation coefficients $\tilde{\lambda}_1(t), \tilde{\lambda}_3(t)$ deviate from the actual macroscopic elongation coefficients $\lambda_1(t)=\exp(-q_3t/2)$, $\lambda_3(t)=\exp(q_3t)$. Affinity of the distribution is a consequence of assumed uniform deformation of $\mathbf{h}$ vectors at any instant of time, t, and induced by the macroscopic elongational flow. The molecular deformation coefficients in Eq. (8), $\tilde{\lambda}_1(t), \tilde{\lambda}_3(t)$, satisfy the following set of equations with the Peterlin modulus $\bar{E}$

$$\tau\frac{\mathrm{d}\tilde{\lambda}_1^2}{\mathrm{d}t} + \left[\bar{E}(t) + q_3\tau\right]\tilde{\lambda}_1^2 - 1 = 0 \tag{9}$$

$$\tau\frac{\mathrm{d}\tilde{\lambda}_3^2}{\mathrm{d}t} + \left[\bar{E}(t) - 2q_3\tau\right]\tilde{\lambda}_3^2 - 1 = 0$$

where $\tau = Na^2/6D$.

It can be easily check, by multiplication of Eq. (7) by x_i^2 and integration, that the coefficients $\tilde{\lambda}_1(t), \tilde{\lambda}_3(t)$ satisfy the following relation, well known for affine chain deformations

$$\langle x_1^2\rangle(t) = \langle x_2^2\rangle(t) = \left(\frac{Na^2}{3}\right)\tilde{\lambda}_1^2(t) \tag{10}$$

$$\langle x_3^2\rangle(t) = \left(\frac{Na^2}{3}\right)\tilde{\lambda}_3^2(t)$$

The initial conditions for Eq. (9) are $\langle x_i^2\rangle(t=0) = Na^2/3$ and $\tilde{\lambda}_i^2(t=0) = 1$. Affinity of the molecular deformation is a consequence of Peterlin approximation which introduces instantaneous linear deformation of chains in the system.

Eq. (8) shows pseudo-affine distribution of chains with molecular elongation coefficients governed by Eq. (9). The evolution equations for the chain elongation coefficients are non-linear and they are coupled since $\bar{E}$ is a function of the average square end-to-end distance, or of $\tilde{\lambda}_1(t), \tilde{\lambda}_3(t)$

$$\langle h^2\rangle(t) = \sum_i \langle x_i^2\rangle(t) = \left(\frac{Na^2}{3}\right)\left[2\tilde{\lambda}_1^2(t) + \tilde{\lambda}_3^2(t)\right] \tag{11}$$

The inverse Langevin function present in Eq. (4) for the Peterlin modulus can be expressed analytically by a Padè approximation [5] in the following form

$$\mathcal{L}^*(x) \cong x\left(\frac{3-x^2}{1-x^2}\right) \tag{12}$$

and this yields the Peterlin modulus

$$\bar{E}(t) = \frac{1}{3} + \frac{2}{3\left[1 - \left(2\tilde{\lambda}_1^2(t) + \tilde{\lambda}_3^2(t)\right)/3N\right]} \tag{13}$$

With the Padè approximation, modulus $\bar{E}$ equals unity at the initial isotropic state, $\tilde{\lambda}_i^2(t=0) = 1$, and it tends to infinity when the average chain conformation approaches full extension, $\langle h^2\rangle(t) \to Na^2$, then $2\tilde{\lambda}_1^2(t) + \tilde{\lambda}_3^2(t) \to 3N$.

3. Analytical approximation for uniaxial elongational flows

For flow deformations dominated by uniaxial elongation, $q_3 > 0$, where we have $q_1 = q_2 = -q_3/2$, time-evolution of the average square end-to-end distance, $\langle h^2\rangle(t)$, is controlled by the elongational component q_3. Then in all conditions, except for the state of rest, we have

$$\langle x_1^2\rangle = \langle x_2^2\rangle < \langle x_3^2\rangle \tag{14}$$

For small elongation rates and/or short deformation times we have $\langle h^2\rangle \ll N^2a^2$ and $\bar{E} \approx 1$. At higher elongation rates and longer deformation times $\langle h^2\rangle \approx \langle x_3^2\rangle$ because $\langle x_1^2\rangle = \langle x_2^2\rangle \ll \langle x_3^2\rangle$. Then, the average $\langle h^2\rangle$ can be approximated by $\langle x_3^2\rangle$, or the trace $2\tilde{\lambda}_1^2(t) + \tilde{\lambda}_3^2(t)$ in Eq. (13) by $\tilde{\lambda}_3^2(t)$, and the Peterlin modulus reduces to

$$\bar{E}(t) \cong \bar{E}\left(\langle x_3^2\rangle(t)\right) = \frac{1}{3} + \left(\frac{2}{3\left[1 - \tilde{\lambda}_3^2(t)/3N\right]}\right) \tag{15}$$

The above form decouples Eq. (9), and functions $\tilde{\lambda}_1(t)$, $\tilde{\lambda}_3(t)$ can be calculated analytically.

Introducing $z = \tilde{\lambda}_3^2$, the decoupled equations read

$$\tau\left(N - \frac{z}{3}\right)\frac{\mathrm{d}z}{\mathrm{d}t} = N + \left[N(2q_3\tau - 1) - \frac{1}{3}\right]z + \frac{1}{9}(1 - 6q_3\tau)z^2 \equiv a + bz + cz^2 \tag{16}$$

$$\tau\frac{\mathrm{d}\tilde{\lambda}_1^2}{\mathrm{d}t} + f(t)\tilde{\lambda}_1^2 - 1 = 0 \tag{17}$$

where

$$a = N, \quad b = N(2q_3\tau - 1) - \frac{1}{3}, \quad c = \frac{1}{9}(1 - 6q_3\tau) \tag{18}$$

$$f(t) = \left(\frac{9N - z(t)}{3[3N - z(t)]}\right) + q_3\tau \tag{19}$$

Since $\Delta = b^2 - 4ac$ is always positive

$$\Delta = \frac{9N^2(2q_3\tau - 1)^2 + 12Nq_3\tau + 2N + 1}{9} \tag{20}$$

solution of Eq. (16) obtained with the initial condition $z(t=0) = 1$ reads

$$-\frac{1}{6c}\ln\left[\frac{a + bz + cz^2}{a + b + c}\right] + \frac{1}{\sqrt{\Delta}}\left(N + \frac{b}{6c}\right)\ln\left[\frac{b + 2cz - \sqrt{\Delta}}{b + 2cz + \sqrt{\Delta}}\,\frac{b + 2c + \sqrt{\Delta}}{b + 2c - \sqrt{\Delta}}\right] = \frac{t}{\tau} \tag{21}$$

Solution of the second Eq. (17) can be obtained after calculation of $z(t)$ from Eq. (21). Then

$$\tilde{\lambda}_1^2(t) = \exp\left[-\int_1^{z(t)} u(z)\mathrm{d}z\right]\left\{1 + \int_1^{z(t)} g(z)\exp\left[\int_1^{z(t)} u(s)\mathrm{d}s\right]\mathrm{d}z\right\} \tag{22}$$

where

$$u(s) = \frac{9N(1 + q_3\tau) - (1 + 3q_3\tau)s}{9(a + bs + cs^2)} \tag{23}$$

$$g(z) = \frac{3N - z}{3(a + bz + cz^2)} \tag{24}$$

4. Uniaxial molecular deformation

Figs. 1–6 illustrate time evolution of the chain elongation coefficients $\tilde{\lambda}_3$ and $\tilde{\lambda}_1$ vs. t/τ calculated from the analytical Eqs. (21) and (22) for the elongation rates $q_3\tau = 0.1$, 0.5, and 0.7, assuming the chain length $N = 100$. The evolution curves predicted by the analytical formulas (solid lines) are

compared in the figures with the numerical solution of Eqs. (9) and (13) also using the Peterlin/Padè approximation (dashed lines). Thin line plots indicate macroscopic elongation coefficients of the viscous medium

$$\lambda_3(t) = \exp(q_3 t), \quad \lambda_1(t) = \exp\left(\frac{-q_3 t}{2}\right) \tag{25}$$

and steady-state, equilibrium limit of the molecular elongation coefficients predicted from the numerical formula [1]

$$\tilde{\lambda}_3((t/\tau)\to\infty) = \left(\frac{1}{\bar{E}_{eq} - 2q_3\tau}\right)^{1/2},$$
$$\tilde{\lambda}_1((t/\tau)\to\infty) = \left(\frac{1}{\bar{E}_{eq} + q_3\tau}\right)^{1/2} \tag{26}$$

where $\bar{E}_{eq}$ is computed from the following self-consistent equation

$$\frac{9N(\bar{E}_{eq} - 1)}{3\bar{E}_{eq} - 1} = \frac{1}{\bar{E}_{eq} - 2q_3\tau} + \frac{2}{\bar{E}_{eq} + q_3\tau} \tag{27}$$

The molecular elongation plots in Figs. 1–6 diverge tangentially from the macroscopic elongation at the initial time, and they approach the equilibrium state at $t/\tau\to\infty$. Such an evolution between macroscopic deformation asymptote and the steady-state one is controlled by the non-linear chain elasticity at the instantaneous state.

The analytical formulas, Eqs. (21) and (22), predict values of the chain elongation coefficients nearly identical with the values obtained numerically from Eq. (9) for $q_3\tau$ above 0.5. Also at the elongation rates $q_3\tau$ below 0.5, the deviation is not significant and the evolution of chain deformation remains within physically sensible bounds. The

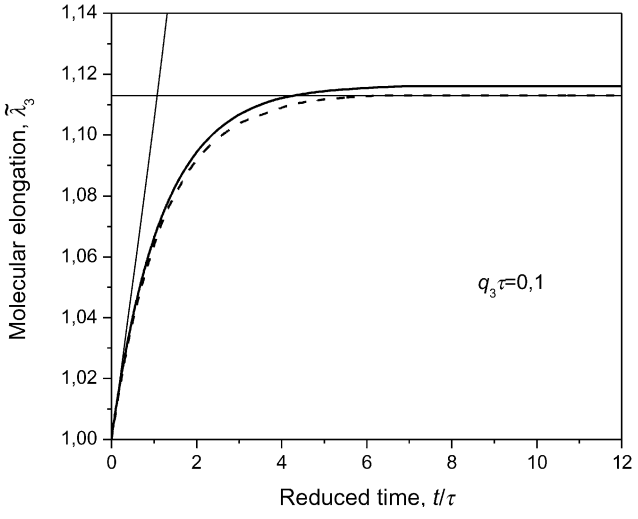

Fig. 1. Molecular elongation $\tilde{\lambda}_3$ vs. reduced time t/τ calculated for uniaxial elongational flow using the analytical Eq. (21) at $q_3\tau = 0.1$ (solid line), and compared with the numerical solution, Eq. (9) (dashed line). Thin lines—macroscopic flow elongation and the steady-state limit of the chain elongation, $N = 100$.

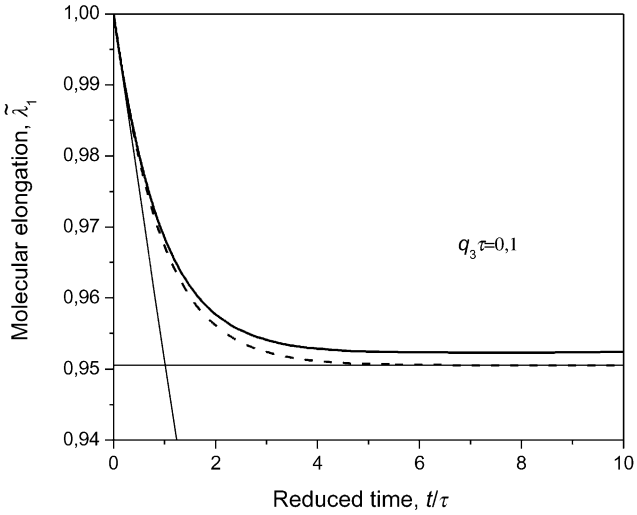

Fig. 2. Molecular elongation $\tilde{\lambda}_1$ vs. reduced time t/τ during calculated for uniaxial elongational flow using Eqs. (21) and (22) at $q_3\tau = 0.1$, and compared with the numerical solution, Eq. (9). Lines like in Fig. 1.

example computations show that the proposed analytical formula can be used for uniaxial elongational flows in a wide range of elongation rates, in particular at faster processes, where very good agreement with the numerical calculations is found.

For comparison, the molecular elongation coefficients predicted by our earlier analytical self-consistent formula [1] deviate more from the numerical predictions, in particular within the range of elongation rates $q_3\tau$ between 0.7 and 5, as well as for intermediate values of the time, $q_3 t$. The deviation of the self-consistent formula leads to an underestimation of the chain elongation. Nevertheless, the self-consistent formula approaches the same steady-state equilibrium limit as the numerical solution does.

It should be mentioned, that the here derived analytical

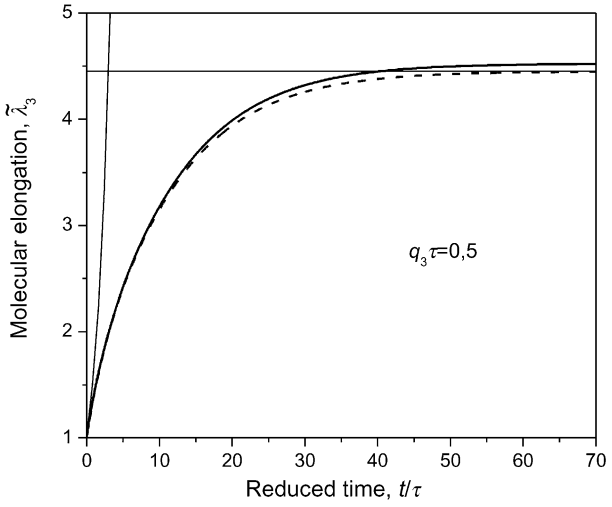

Fig. 3. Molecular elongation $\tilde{\lambda}_3$ vs. reduced time t/τ calculated for uniaxial elongational flow using the analytical Eq. (21) at $q_3\tau = 0.5$, and compared with the numerical solution, Eq. (9). Lines like in Fig. 1.

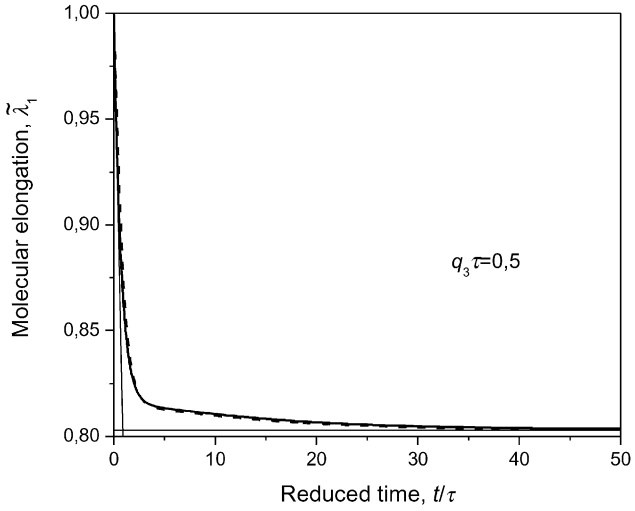

Fig. 4. Molecular elongation $\tilde{\lambda}_1$ vs. reduced time t/τ calculated for uniaxial elongational flow using Eqs. (21) and (22) at $q_3\tau=0.5$, and compared with the numerical solution, Eq. (9). Lines like in Fig. 1.

formulas are valid solely for the uniaxial elongational flow. The new analytical solution is possible only when the Peterlin modulus is mainly controlled by a single, dominating chain deformation coefficient, as it is in the case of elongational flow. Then, the modulus can be approximated by a function of the dominating deformation coefficient alone, and the set of differential equations decouples and can be solved analytically. This allows the new analytical solution of the decoupled equations, avoiding the less exact self-consistent approach.

The decoupling is not possible for biaxial deformation, where two of the deformation coefficients are of the same order and none of them can be neglected.

Fig. 7 shows time evolution of the molecular elongation $\tilde{\lambda}_3$ predicted by the present analytical formula, Eq. (21), vs.

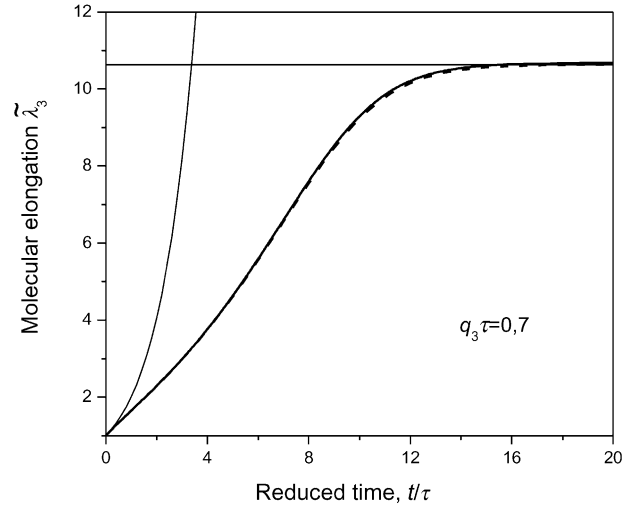

Fig. 5. Molecular elongation $\tilde{\lambda}_3$ vs. reduced time t/τ calculated for uniaxial elongational flow using Eq. (21) for $q_3\tau=0.7$, and compared with the numerical solution, Eq. (9). Lines like in Fig. 1. The analytical and numerical solutions nearly overlap.

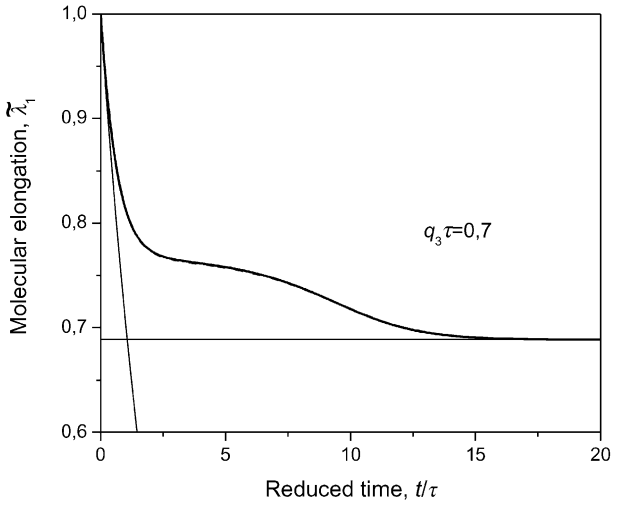

Fig. 6. Molecular elongation $\tilde{\lambda}_1$ vs. reduced time t/τ calculated for uniaxial elongational flow from Eqs. (21) and (22) for $q_3\tau=0.7$, and compared with the numerical solution, Eq. (9). Lines like in Fig. 1. The analytical and numerical solutions nearly overlap.

macroscopic elongation $\lambda_3=\exp(q_3t)$ for several elongation rates $q_3\tau$ between 0.1 and 50. The molecular elongation plots (solid lines) deviate from the affine macroscopic elongation (dashed line) the later, the higher is the elongation rate. At the fastest process, $q_3\tau=50$, the molecular elongation coefficient follows the macroscopic one, until achieving the equilibrium limit with nearly extended chains.

5. Stress and molecular orientation

In the Peterlin approximation, time evolution of the

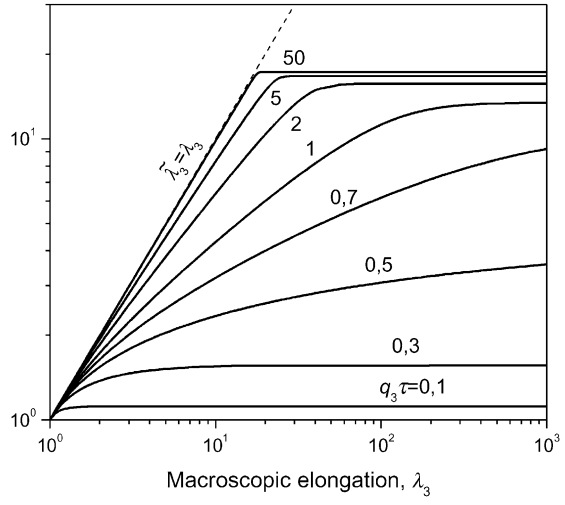

Fig. 7. Evolution of the affine molecular elongation, $\tilde{\lambda}_3$, in the uniaxial elongational flow calculated using the analytical formula, Eq. (21), vs. macroscopic elongation λ_3 at several elongation rates $q_3\tau$ (solid lines). Dashed line—the limit of the molecular deformation following exactly the macroscopic flow, $N=100$.

elastic force between the chain ends is controlled by the evolution of the average square end-to-end distance, $\langle h^2(t)\rangle$

$$\mathbf{f}_{\mathrm{el}}(t) \cong \frac{3kT}{Na^2}\bar{E}(\langle h^2\rangle(t))\mathbf{h} \tag{28}$$

The average elastic stress tensor reads [6,7]

$$\langle \mathbf{p}\rangle(t) = \nu\langle \mathbf{f}_{\mathrm{el}} \otimes \mathbf{h}\rangle \cong 3\nu kT\bar{E}(t)\left(\frac{\langle \mathbf{h}\otimes\mathbf{h}\rangle(t)}{Na^2}\right)$$

$$= \frac{kT\bar{E}(t)}{v_0}\frac{\tilde{\mathbf{\Gamma}}(t)}{N} \tag{29}$$

where ν is number density of chains, $v_0 = 1/\nu N$—volume per single segment in the system, and

$$\tilde{\mathbf{\Gamma}}(t) = \begin{bmatrix} \tilde{\lambda}_1^2(t) & 0 & 0 \\ 0 & \tilde{\lambda}_1^2(t) & 0 \\ 0 & 0 & \tilde{\lambda}_3^2(t) \end{bmatrix} \tag{30}$$

is a time-dependent molecular deformation tensor in the uniaxial flow. In the Gaussian limit we have $\bar{E} = 1$, and the stress tensor reduces to

$$\langle \mathbf{p}\rangle(t) = \frac{kT}{v_0 N}\tilde{\mathbf{\Gamma}}(t) \tag{31}$$

Then, the non-linear elastic tensile stress reads

$$\langle \Delta p\rangle(t) = \langle p_{33} - p_{11}\rangle \cong \frac{kT\bar{E}(t)}{v_0 N}\left(\tilde{\lambda}_3^2(t) - \tilde{\lambda}_1^2(t)\right) \tag{32}$$

where the modulus $\bar{E}(t)$ in the Peterlin/Padè approximation is a function of $\tilde{\lambda}_1(t)$, $\tilde{\lambda}_3(t)$, (Eq. (13)), and it tends to infinity at the full chain extension, $\mathrm{tr}\tilde{\Gamma} = \tilde{\lambda}_3^2 + 2\tilde{\lambda}_1^2 = 3N$.

Evolution of the Peterlin modulus $\bar{E}$ with the macroscopic deformation $\ln\lambda_3 = q_3 t$ predicted from the analytical solution, Eqs. (15) and (21), is shown in Fig. 8 for several elongation rates, $q_3\tau$, between 0.1 and 50. Initial conditions of an isotropic, unstressed system are assumed. Substantial effects of the flow deformation on the modulus are predicted for flow rates much exceeding 0.5. Below that value the effects are negligible. Macroscopic elongation λ_3 at which the modulus approaches its steady-state value is the lower, the higher is the elongation rate. Saturation of the modulus at the steady-state molecular elongation increases by approximately ten times with increasing $q_3\tau$ to a value of five, and by one hundred times at $q_3\tau = 50$.The modulus tends to infinity at full chain extension with $q_3\tau \to \infty$.

Orientation of chain segments, **a**, in a chain with end-to-end vector **h** is represented by the following orientation tensor [2,8]

$$\mathbf{A}(\mathbf{h}) = \left[1 - \frac{3\left(\frac{h}{Na}\right)}{\mathcal{L}^*\left(\frac{h}{Na}\right)}\right]\frac{\mathbf{h}\otimes\mathbf{h}}{h^2} \tag{33}$$

In the Gaussian limit of small chain extensions, $h/Na \ll 1$, we have [2]

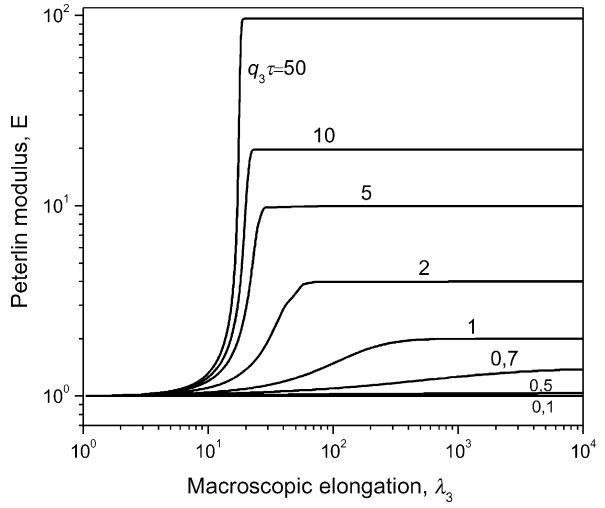

Fig. 8. Evolution of the Peterlin modulus, $\bar{E}$, in the uniaxial elongational flow vs. macroscopic elongation, λ_3, calculated from Eq. (13) using molecular elongation coefficients calculated from the analytical formula, Eqs. (21) and (22), for several elongation rates, $q_3\tau$. $N = 100$.

$$\mathbf{A}(\mathbf{h}) = \frac{3}{5}\frac{\mathbf{h}\otimes\mathbf{h}}{N^2a^2} \tag{34}$$

and the average orientation tensor

$$\langle \mathbf{A}\rangle = \frac{1}{5}\frac{\tilde{\mathbf{\Gamma}}}{N} \tag{35}$$

Eqs. (31) and (35) provide well known linear stress-orientation relation for Gaussian systems.

At higher chain extensions, with the Peterlin approximation for a chain in the system

$$\frac{\mathcal{L}^*\left(\frac{h}{Na}\right)}{3\left(\frac{h}{Na}\right)} \cong \bar{E}(\langle h^2\rangle) \tag{36}$$

we have

$$\mathbf{A}(\mathbf{h}) \cong \left(1 - \frac{1}{\bar{E}}\right)\frac{\mathbf{h}\otimes\mathbf{h}}{h^2} \tag{37}$$

The above formula is valid in the entire range of chain extension, and the average orientation tensor reads

$$\langle \mathbf{A}\rangle \cong \left(1 - \frac{1}{\bar{E}}\right)\left\langle\frac{\mathbf{h}\otimes\mathbf{h}}{h^2}\right\rangle \tag{38}$$

With increasing the modulus $\bar{E}$ to infinity (nearly extended chains) the average tensor $\langle \mathbf{A}\rangle$ converges to the diadic form $\langle \mathbf{h}\otimes\mathbf{h}/h^2\rangle$ well known for rigid-rod molecules.

For uniaxial deformations, the axial components of $\langle \mathbf{A}\rangle$ read

$$\langle A_{11}\rangle = \langle A_{22}\rangle$$

$$\cong \frac{1}{4\pi}\left(1 - \frac{1}{\bar{E}}\right)\int_0^{2\pi} \mathrm{d}\varphi \int_0^{\pi} \frac{\tilde{\lambda}_1^2 \sin^3\vartheta \cos^2\varphi}{r^2(\vartheta,\varphi)}\mathrm{d}\vartheta \tag{39}$$

$$\langle A_{33}\rangle \cong \frac{1}{4\pi}\left(1-\frac{1}{\tilde{E}}\right)\int_0^{2\pi} d\varphi \int_0^{\pi} \frac{\tilde{\lambda}_3^2 \cos^2\vartheta}{r^2(\vartheta,\varphi)} \sin\vartheta \, d\vartheta$$

where

$$r^2(\vartheta,\varphi) = \tilde{\lambda}_1^2 \sin^2\vartheta + \tilde{\lambda}_3^2 \cos^2\vartheta \tag{40}$$

Usually, axial orientation of chain segments with respect flow direction ($i=3$) is usually characterized by the orientation factor, f_3, which can be determined from the difference of the axial components [2]

$$f_3 = \langle A_{33}\rangle - \langle A_{11}\rangle \tag{41}$$

In the Gaussian limit, the orientation factor reduces to the known formula

$$f_3 = \frac{1}{5N}\left(\tilde{\lambda}_3^2 - \tilde{\lambda}_1^2\right) \tag{42}$$

For non-linear systems, the components $\langle A_{11}\rangle$ and $\langle A_{33}\rangle$ can be calculated from Eq. (39) valid for the case $\tilde{\lambda}_3 > \tilde{\lambda}_1$, and they read

$$\langle A_{11}\rangle = -\frac{1}{2}\left(1-\frac{1}{\tilde{E}}\right)\frac{\tilde{\lambda}_3^2}{\tilde{\lambda}_3^2-\tilde{\lambda}_1^2} \times \left[\frac{\tilde{\lambda}_1^2}{\tilde{\lambda}_3^2} - \frac{\tilde{\lambda}_1^2}{\sqrt{\tilde{\lambda}_1^2\left(\tilde{\lambda}_3^2-\tilde{\lambda}_1^2\right)}} \operatorname{arctg}\sqrt{\frac{\tilde{\lambda}_3^2}{\tilde{\lambda}_1^2}-1}\right] \tag{43}$$

$$\langle A_{33}\rangle = \left(1-\frac{1}{\tilde{E}}\right)\frac{\tilde{\lambda}_3^2}{\tilde{\lambda}_3^2-\tilde{\lambda}_1^2} \times \left[1 - \frac{\tilde{\lambda}_1^2}{\sqrt{\tilde{\lambda}_1^2\left(\tilde{\lambda}_3^2-\tilde{\lambda}_1^2\right)}} \operatorname{arctg}\sqrt{\frac{\tilde{\lambda}_3^2}{\tilde{\lambda}_1^2}-1}\right]$$

Then, time evolution of the orientation factor f_3, calculated with the Peterlin/Padè approximation, reads

$$f_3(t) = \frac{2\tilde{\lambda}_3^2\left(\tilde{\lambda}_3^2+2\tilde{\lambda}_1^2\right)}{\left(9N-\tilde{\lambda}_3^2-2\tilde{\lambda}_1^2\right)\left(\tilde{\lambda}_3^2-\tilde{\lambda}_1^2\right)} \times \left[1 + \frac{\tilde{\lambda}_1^2}{2\tilde{\lambda}_3^2} - \frac{3\tilde{\lambda}_1^2}{2\sqrt{\tilde{\lambda}_1^2\left(\tilde{\lambda}_3^2-\tilde{\lambda}_1^2\right)}} \operatorname{arctg}\sqrt{\frac{\tilde{\lambda}_3^2}{\tilde{\lambda}_1^2}-1}\right] \tag{44}$$

where the time-dependent chain elongation coefficients $\tilde{\lambda}_3 > \tilde{\lambda}_1$ can be calculated from the analytical Eqs. (21) and (22).

Figs. 9 and 10 illustrate evolution of the reduced tensile stress, $\langle \Delta p\rangle v_0/kT$, and the axial orientation factor, f_3, with increasing macroscopic deformation λ_3 at several elongation rates. The stress and the orientation factor are computed from Eqs. (32) and (34) using the molecular elongation coefficients predicted form the analytical solution, Eqs. (21) and (22), for isotropic, unstressed initial conditions. The calculated tensile stress approaches a steady-state limit, and the limit level increases by orders of magnitude with increasing the elongation rate, in particular for faster processes, $q_3\tau > 0.5$. The increase of the stress is unlimited when increasing molecular deformation up to full chain extension at the limit of $q_3\tau \to \infty$. The orientation factor f_3 also shows a steady-state plateau at the equilibrium stress, and the values of f_3 are limited by unity when the tensile stress increases to infinity. This implies non-linear stress-orientation behaviour of the system at high stresses.

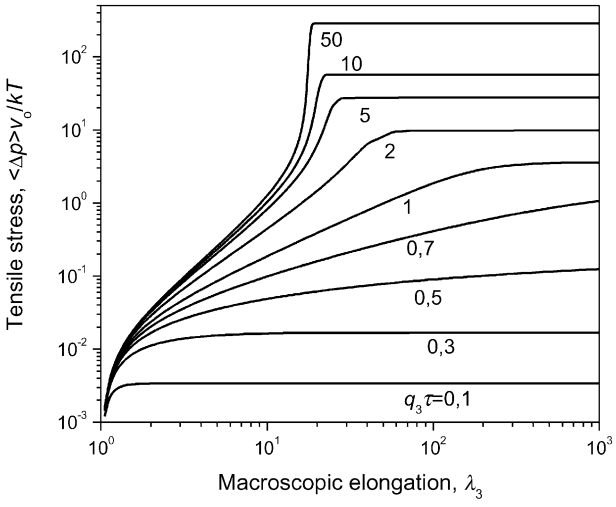

Fig. 9. Evolution of the reduced tensile stress, $\langle \Delta p\rangle v_0/kT$, in the uniaxial elongational flow vs. macroscopic elongation, λ_3, calculated using Eq. (32) using molecular elongation coefficients calculated from the analytical formula.

Fig. 11 shows the orientation factors f_3 plotted vs. the reduced tensile stress, $\Delta p v_0/kT$, calculated for different

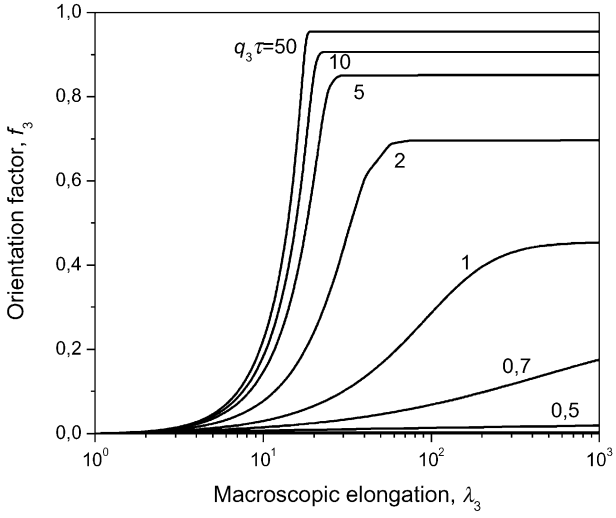

Fig. 10. Evolution of the axial orientation factor, f_3, in uniaxial elongational flow vs. macroscopic elongation, λ_3, calculated using Eq. (44) using molecular elongation coefficients calculated from the analytical formula.

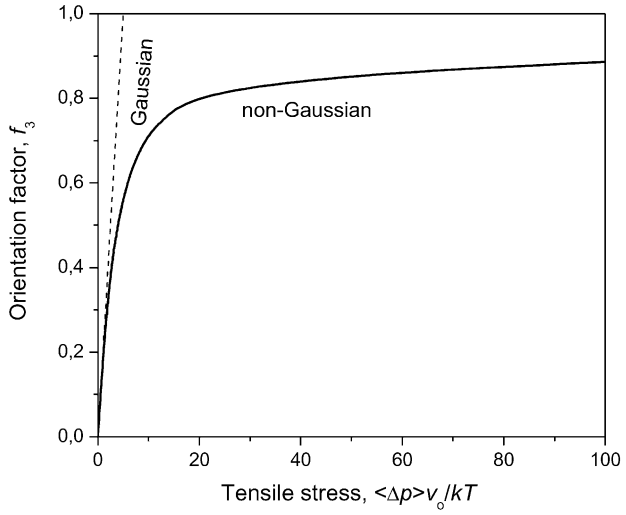

Fig. 11. Axial orientation factor, f_3, vs. reduced tensile stress, $\langle\Delta p\rangle v_0/kT$, in the uniaxial elongational flow calculated using Eqs. (21), (22), (32) and (44) using molecular elongation coefficients calculated from the analytical formula in a wide range of elongation rates and stresses (solid line). Dashed line—Gaussian approximation, $N=100$.

elongation rates from the analytical formulas. The values coincide in a single stress-orientation plot in the entire range of the elongation rates used in the calculations. The dashed line indicates the Gaussian behaviour. The non-linear plot predicted by the present analytical formula deviates from the Gaussian plot approximately at the level of the orientation factor of about 0.2.

Axial orientation factor, f_3, predicted by the present analytical formula is compared in Fig. 12 with experimental measurements of the amorphous orientation factor [9–13] and the average chain elongation in PET fibers from the measurements of the elongation at break. Assuming that the product of the actual chain elongation coefficient in a fiber, $\tilde{\lambda}_{\text{fiber}}$, and the elongation at break, λ_{break}, should be a constant representing maximum chain elongation at break, we have

$$\tilde{\lambda}_{\text{fiber}}\lambda_{\text{break}} = \tilde{\lambda}_{\max} = \text{const} \tag{45}$$

Then, the reduced elongation coefficient $\tilde{\lambda}_{\text{fiber}}/\tilde{\lambda}_{\max}$ can be expressed by the inverse of the elongation at break, $1/\lambda_{\text{break}}$.

Solid line in Fig. 12 shows axial orientation factor f_3 vs. the reduced molecular elongation $\tilde{\lambda}_3/\tilde{\lambda}_{3,\max}$ computed from the molecular elongation coefficients determined form Eqs. (21) and (22). In this calculations we have $\tilde{\lambda}_{3,\max}=\sqrt{3N}$, and the initial condition $\langle x_1^2\rangle(t=0)=\langle x_3^2\rangle(t=0)=Na^2/3$. The plot calculated vs. reduced chain elongation coefficient $\tilde{\lambda}_3/\tilde{\lambda}_{3,\max}$ is compared in the figure with the experimental measurements of the amorphous orientation factor vs. $1/\tilde{\lambda}_{\text{break}}$. The experimental points deviate from the model prediction at higher chain elongations and orientation. The deviation can be a consequence of highly oriented crystallites present in fibers exhibiting high amorphous orientation. The crystallites may disturb the network of entanglements and introduce confined spaces for the amorphous segments. The highest values of the amorphous orientation factor and chain elongation are measured for as-spun fibers obtained by hot-tube melt spinning [10,11]. The fibers show the degree of crystallinity of about 30% and high crystalline orientation.

Contribution of the elastic tensile stress to the apparent elongational viscosity, $\langle\Delta p\rangle/q_3$, calculated from this model is shown in Fig. 13. The figure shows time-evolution of the contribution calculated for several elongation rates. It is seen that in the range of low elongation rates, $q_3\tau<0.5$, the deformed chains contribute to the viscosity a term nearly proportional to time at the beginning of the process which levels off to a steady-state value. At higher elongation rates, a steep increase followed by levelling off at the steady-state

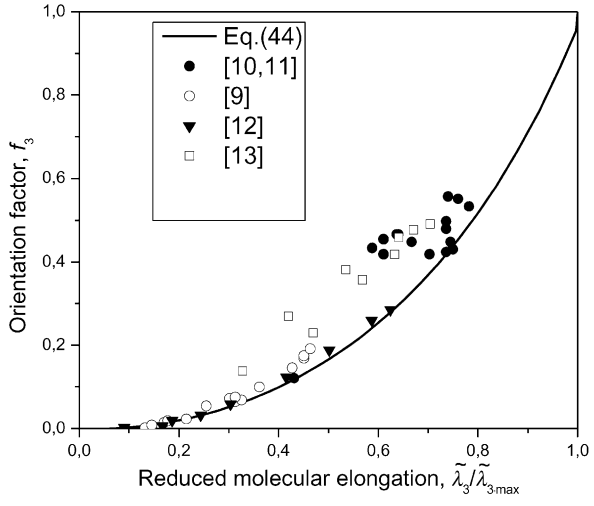

Fig. 12. Axial orientation factor, f_3, plotted vs. reduced molecular elongation coefficient $\tilde{\lambda}_3/\tilde{\lambda}_{3,\max}$, calculated using the analytical solution, Eqs. (21), (22) and (44), and compared with the experimental results.

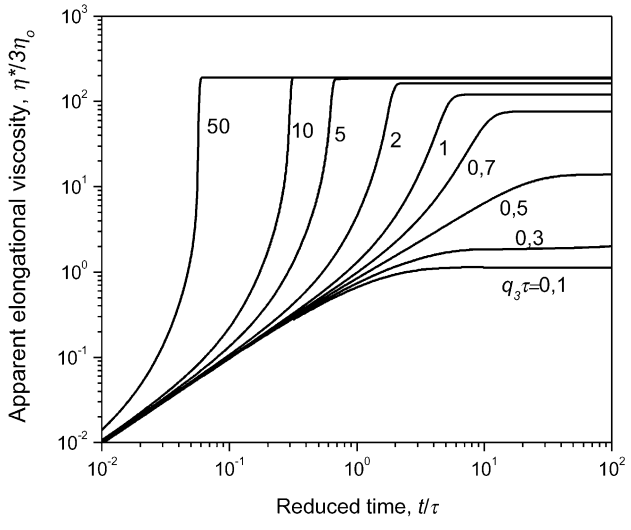

Fig. 13. Reduced elongational viscosity, $\eta^*/3\eta_0=\langle\Delta p\rangle Nv_0/3kT\tau q_3$, vs. reduced time, t/τ, calculated using the analytical solution, Eqs. (21), (22) and (32), for several elongation rates $q_3\tau$. η^*—elongational viscosity, η_0—Newtonian shear viscosity, $N=100$.

is predicted. The steady-state level increases by orders of magnitude with increasing $q_3\tau$. Similar behaviour during the elongation time has been shown by measurements of the apparent elongational viscosity in polypropylene melt subjected to constant strain rates [14,15].

6. Conclusions

Solution of the evolution Eq. (7) for the system of non-Gaussian chains subjected to uniaxial elongational flow with Peterlin approximation for the chain elasticity is an affine, time-dependent distribution function of the chain end-to-end-vectors, $W(\mathbf{h},t)$, Eq. (8). Components of the affine molecular deformation tensor, or the chain elongation coefficients, are governed by the system of non-linear evolution Eq. (9), coupled by the time-dependent Peterlin modulus $\bar{E}(t)$. The Peterlin modulus equals unity for the system of unstressed, relaxed chains and tends to infinity for the system of fully extended chains. Analytical solution of the evolution equations is found in this paper, Eqs. (21) and (22), with the assumption of dominating elongational component in the applied external uniaxial flow field. With such assumption, the evolution Eq. (9) is decoupled and solved analytically with Padè approximation for the inverse Langevin function.

Affine form of the evolution of the distribution function $W(\mathbf{h},t)$ during the flow is a consequence of linear form of the chain elastic force with respect to vectors $\mathbf{h}$ in the Peterlin approximation, while the instantaneous modulus of each chain in the system is expressed by inverse Langevin function of an average chain extension.

The affine molecular deformation tensor, $\tilde{\mathbf{\Gamma}}$, deviates from the macroscopic affine deformation tensor during the deformation time. Symmetry of molecular deformation tensor results from symmetry of the applied flow. The analytical solution shows physically sensible asymptotic behaviour for uniaxial elongational flows with dominating elongational component and small deviation from numerical predictions. The deviation is negligible at higher elongation rates, $q_3\tau > 0.5$. The analytical solution can be also used at lower elongation rates with preserved physical sense of the results, for example for elongation rates $q_3\tau > 0.3$. At lower elongation rates, Gaussian limit is available.

At the beginning of the evolution process, the analytical solution, as well as the numerical one, is tangential to the macroscopic elongational deformation, next it deviates with increasing the processing time, and converges to a steady-state, equilibrium limit. The non-linear analytical model is valid for the entire range of elongation rates and chain extensions in uniaxial elongational flows.

The affine evolution of the distribution function in non-linear systems enables calculations of time evolution of average functions and tensors such as free energy, stress, orientation, etc. The analytical formula is applied for example calculations of the evolution of molecular elongation coefficients during time, and versus macroscopic elongation applied to the sample in a wide range of elongation rates and deformation times. Evolution of tensile stress, axial orientation factor, and apparent elongational viscosity is also calculated using the analytical formula.

A unique master plot representing non-linear stress-orientation behaviour is also calculated, and the results are compared with experimental measurements of the amorphous orientation factor vs. elongation at break of PET fibers. The comparison indicates physically sensible predictions of the analytical formula proposed for non-linear systems subjected to uniaxial elongational flow with dominating elongational component.

Acknowledgements

The research was done within the COST P12 cooperation programme, and it was supported in part by grant for scientific cooperation from the Polish Ministry of Scientific Research and Information Technology.

References

[1] Ziabicki A, Jarecki L, Schoene A. Polymer 2004;45:5735.
[2] Jarecki L, Ziabicki A. Polymer 2002;43:2549.
[3] Jarecki L, Ziabicki A. Polymer 2002;43:4065.
[4] Peterlin A. Polym Lett 1966;4:287.
[5] Cohen A. Rheol Acta 1991;30:270.
[6] Ziabicki A. Proceedings of the fifth international congress on rheology. vol. 3. Kyoto: University of Tokyo Press; 1970. p. 235.
[7] Ziabicki A, Jarecki L. Colloid Polym Sci 1986;264:343.
[8] Zimm BH. J Chem Phys 1956;24:269.
[9] King CM. Appl Polym Symp 1991;47:171.
[10] Mercurio F. PhD Thesis. High-speed melt spinning of polyester fibers. Spinning conditions—structure—properties correlations, University of Genova, Italy; 1997.
[11] Blim A, Oldak E, Wasiak A, Jarecki L. Polymer 2005;50:48.
[12] Long SD, Ward IM. J Appl Polym Sci 1990;42:1911.
[13] Schmack G. Leibniz Institute of Polymer Research Dresden [private information].
[14] Ishizuka O, Koyama K. Polymer 1980;21:164.
[15] Bird RB, Armstrong RC, Hassager O. Dynamics of polymeric liquids. vol. 1. New York: Wiley; 1987 p. 135.